

Forced expression of Nanog in hematopoietic stem cells results in a $\gamma\delta$ T-cell disorder

Yosuke Tanaka¹, Takumi Era¹, Shin-ichi Nishikawa,^{1,2} and Shin Kawamata^{1,2}

¹Riken Center for Developmental Biology, Kobe, Japan; ²Foundation for Biomedical Research and Innovation, Kobe, Japan

Nanog is a key molecule involved in the maintenance of the self-renewal of undifferentiated embryonic stem (ES) cells. In this work we investigate whether Nanog can enhance self-renewal in hematopoietic stem cells. Contrary to our expectation, no positive effect of Nanog transduction was detected in bone marrow reconstitution assays. However, recipients of *Nanog*-transduced (Nanog) hematopoietic stem cells (HSCs) invariably

develop a unique disorder typified by an atrophic thymus occupied by Nanog-expressing $\gamma\delta$ T-cell receptor-positive (TCR⁺) cells (Nanog T cells). All thymi are eventually occupied by Nanog T cells with CD25⁺CD44⁺ surface phenotype that home selectively to the thymus on transfer and suppress normal thymocyte development, which is partly ascribed to destruction of the microenvironment in the thymus cortex. Moreover, this initial disorder

invariably develops to a lymphoproliferative disorder, in which Nanog T cells undergo unlimited proliferation in the peripheral lymphoid tissues and eventually kill the host. This invariable end result suggests that Nanog is a candidate oncogene for $\gamma\delta$ T-cell malignancy. (Blood. 2007;110:107-115)

© 2007 by The American Society of Hematology

Introduction

The self-renewal capacity and multipotency of embryonic stem (ES) cells can easily be maintained in culture. Several molecules have been implicated in the maintenance of these essential features of ES cells. Oct3/4 in association with the high mobility group (HMG) factor Sox2 is reported to be essential for self-renewal of ES cells,¹⁻³ and forced Nanog expression can maintain the immature state of ES cells in a LIF-Stat3-independent manner.^{4,5} However, the exact molecular mechanism underlying the maintenance of the stem cell state is yet to be elucidated.

Several reports have suggested that the core factors maintaining ES self-renewal can affect the activity of other stem cells. For example, Oct3/4 is expressed in mesenchymal stem cells derived from CD133⁺ cells in mobilized peripheral blood and cord blood.⁶ Nanog was also shown to be expressed in circulating CD14⁺CD34^{low} endothelial cells.⁷

Although the role of these molecules in adult tissue stem cells remains unclear, it has been expected that it may be possible to use them to enhance the self-renewal of tissue stem cells. This expectation is supported by the recent report of Hochedlinger et al⁸ showing that Oct3/4 overexpression enhances the proliferation of tissue stem cells.

Compared with ES cells, it has been difficult to maintain the self-renewal of unmanipulated hematopoietic stem cells in vitro, although forced expression of HoxB4 or activated β -catenin confers enhanced self-renewal to hematopoietic progenitor cells (HPCs) in vitro.^{9,10} Hence, it is worthwhile to determine whether the molecules involved in the self-renewal of ES cells can enhance that of HPCs. The initial aim of this work was to evaluate the effect of ectopic expression of Nanog on the behavior of hematopoietic stem cells. Although this expectation was not the case, we report here that Nanog overexpression induces an unusual $\gamma\delta$ T-cell

receptor-positive (TCR⁺) cell type that destroys the microenvironment of the thymus and eventually develops to a malignant lymphoproliferative disorder.

Materials and methods

The study protocol was approved by an institutional review board of Riken Center for Developmental Biology and the Foundation of Biomedical Research and Innovation.

Infection procedure

Mouse whole bone marrow (BM) cells were isolated from 4-week-old C57BL/6CrSlc mice (Shimizu Laboratory Supplies, Kyoto, Japan) treated with intravenously administered 150 mg 5-fluorouracil/kg (Sigma Aldrich Japan, Tokyo, Japan) 5 days before being humanely killed. To purify the mouse stem cell population, lineage depletion from whole BM was performed with Lineage depletion kit (Miltenyi Biotec, Bergisch Gladbach, Germany) and the AutoMACS device (Miltenyi Biotec) in accordance with the manufacturer's instructions. After lineage depletion, the Sca-1/c-Kit (BD Pharmingen, San Diego, CA) positive fraction was purified using a fluorescence-activated cell sorting (FACS) Aria sorter (BD Biosciences, San Jose, CA). The sorted cells were cultured for 12 to 24 hours for recovery before retroviral infection.

A cDNA for mouse *Nanog* (Gene Bank Accession No. XM132755, nucleotide sequence 91–933) was subcloned into the retrovirus vector pMSCV-IRES-eGFP (Mie: control vector). pMSCV-Nanog-IRES-eGFP (Mie-Nanog) and pMSCV-IRES-eGFP (Mie) were transfected into 293T cells for retroviral production. Retroviral transduction into KSL cells was performed as described elsewhere.^{11,12} Gene transduction efficiency was determined by eGFP expression using flow cytometry on a FACS Calibur (BD Bioscience) before mouse bone marrow reconstitution.

Submitted August 1, 2006; accepted March 11, 2007. Prepublished online as *Blood* First Edition Paper, March 14, 2007; DOI 10.1182/blood-2006-08-039628.

The publication costs of this article were defrayed in part by page charge

payment. Therefore, and solely to indicate this fact, this article is hereby marked "advertisement" in accordance with 18 USC section 1734.

© 2007 by The American Society of Hematology

Bone marrow reconstitution

Eight-week-old C57BL/6CrSlc mice were purchased (Shimizu Laboratory Supplies) and maintained in the CDB animal facility in compliance with animal care regulations and rules at CDB Kobe, Japan. Mice were irradiated with 9.5 Gy followed by tail vein injection of 2×10^4 mock (empty vector)- or Nanog-transduced KSL cells together with 1×10^5 rescue whole BM cells as described elsewhere.¹³ BM reconstituted mice were maintained in the CDB animal facility and fed with 25mg kanamycin sulfate/L (Meiji Pharma, Tokyo, Japan) water for a week after BM transplantation.

Flow cytometry analysis

Cell lineages were determined by staining with phycoerythrin (PE)-Mac-1 (M1/70), allophycocyanin (APC)-Gr-1 (RB6-8C5), fluorescein isothiocyanate (FITC)-c-Kit (2B8), PE-Sca-1 (D7), PE-CD3 (17A2), PE-CD4 (GK1.5), PE-CD8a (53-6.7), PE- γ TCR (GL3), APC-CD19 (1D3), APC- α TCR (H57-597), APC-CD8a (53-6.7), APC-CD44 (IM7), APC-c-Kit (2B8), and biotinylated (biotin)-CD25 (7D4). All antibodies were purchased from BD Pharmingen and stained in accordance with the manufacturer's recommended protocol. For FACS analysis of thymocytes, we analyzed the population after gating out cells expressing CD19, Ter119, Mac1, or Gr1.

Immunohistologic analysis of thymus sections

Paraformaldehyde-fixed tissues were embedded in paraffin. Sections 8- μ m thick were stained with hematoxylin and eosin. Frozen sections were fixed with cold acetone and stained with the following antibodies: anti-integrin β 1 (KMI6; BD Pharmingen), anti-integrin β 7 (M293; BD Pharmingen), anti-integrin α 4 (Ha31/8; BD Pharmingen), ER-TR4, ER-TR5 (gifts from Dr Amagai, Meiji College of Oriental Medicine),¹⁴ and anti-Nanog (ReproCell, Kyoto, Japan) antibodies. These antibodies were visualized with secondary antibodies (Alexa 488-conjugated anti-rabbit donkey IgG [Molecular Probes, Eugene OR] or Cy3-conjugated anti-rat donkey IgG [Jackson Laboratory, Bar Harbor ME]). Sections were mounted with VECTASHILD with DAPI (Vector Laboratories, Burlingame, CA). Images were acquired using an Olympus IX81 microscope system and 4×0.13 (Figure 2B right and left panels; Figure 2C lower panels) or 10×0.40 (Figure 2B middle panel; Figure 2C upper panels; Figure 2E; Figure 6B right and middle panels, and Figure 6C) objectives (Olympus, Tokyo, Japan) and processed using Adobe Photoshop 6.0 (Adobe Systems, San Jose, CA).

Quantitative RT-PCR analysis

Total RNA was extracted from cultured cells and respective mouse tissues with the RNeasy kit or RNeasy Micro kit (Qiagen Japan, Tokyo, Japan) and cDNA synthesis was performed with SuperScript II reverse transcriptase (RT; Invitrogen Japan, Tokyo, Japan) in accordance with the manufacturer's instructions. Expression of marker genes was evaluated with real-time polymerase chain reaction (PCR) using SYBR Green (Applied Biosystems Japan, Tokyo Japan). The following primer pairs were used: GAPDH forward, 5'-AGGTCGGTGTGAACGGATTG-3', reverse, 5'-TGTAGACCATGT AGTTGAGGTCA-3'; Nanog forward, 5'-TCTTCC-TGGTCCCCACAGTTT-3', reverse, 5'-GCAAGAATGTTCTCGGG-ATGAA-3'; β -actin forward, 5'-GGCTGTATCCCCTCCATCG-3', reverse, 5'-CCAG TTGGTAACAATGCCATGT-3'; HES1 forward, 5'-ATAGCTC-CCGGCATTCCAAG-3', reverse 5'-GCGCGGTATTTCCCAACA-3'; Oct3/4 forward, 5'-AGTTGGCGTGGAGACTTTGC-3', reverse, 5'-CAGGG-CTTTCATGTCCTGG-3'; Sox2 forward, 5'-GCGGAGTGGAACTTTT-GTCC-3', reverse 5'-CGGAAGCGTGTACTTATCCTT-3'.

OP9/OP9-DL1 coculture

OP9 stromal cell lines were obtained from the Riken Bio-Resource Center (BRC, Tsukuba, Japan) and were maintained in α MEM (Invitrogen Japan) supplemented with 20% fetal bovine serum (JRH Biosciences, Lenexa, KS) and 50 μ M 2-ME (Sigma Aldrich Japan, Tokyo, Japan). Murine *Delta-like 1* cDNA (Dl1; Gene Bank Accession No. NM_007865, 348-2516) was cloned from E8.5 embryo RNA by reverse transcription-polymerase chain

reaction and subcloned into the retroviral vector pMSCV-IRES-DsRED (MiD) for transduction to OP9 cells. *Dl1*-transduced OP9 cells were sorted for DsRED expression twice with a FACS Aria sorter to make the OP9-MiD-Dl1 (referred to as OP9-DL1) cell line. Empty vector MiD-transduced OP9 stable cell line OP9-MiD (referred to as OP9 control) was used as a control. OP9 control and OP9-DL1 stromal cells were cultured as described elsewhere.¹⁵ For competition assays, 10^4 wild-type DN thymocytes and 10^4 Nanog-transduced thymocytes (Nanog T) were mixed and cocultured on OP9-DL1 in 6-well plates in the presence of 5 ng Flt3L/mL (PeproTech, London, United Kingdom) and 5 ng IL-7/mL (PeproTech). Cells were collected for cell number and FACS analysis at day 10 and day 14.

Cytotoxic assay

For FACS analysis, 10^4 , 2.5×10^4 , and 5.0×10^4 cells of wild-type DN thymocytes or Nanog T cells were seeded in the well of 12-well culture plates containing 2×10^5 OP9 or OP9-DL1 cells, respectively. After 5 days of culture, the cells were harvested and enumerated using propidium iodide (PI). The proportion of dead cells was determined from the number of PI-stained cells and total cell numbers.

Western blotting

Wild-type DN thymocytes and Nanog T cells were cocultured on OP9-DL1 with DMSO (mock treated) or 1 μ M DAPT (Calbiochem, San Diego, CA). Cell lysates were fractionated through sodium dodecyl sulfate-polyacrylamide gel electrophoresis (SDS-PAGE) and then transferred to PDVF. Intracellular Notch1 was detected with Cleaved Notch 1(Val 1744) Antibody (Cell Signaling Technology, Beverly, MA).

Southern blotting

Southern blotting was performed using DIG High Prime DNA Labeling and Detection starter kit II (Roche Diagnostic GmbH, Penzberg, Germany). Genomic DNA (5 μ g) was digested with *Eco*RI and hybridized with the *egfp* probe, which is isolated from the MSCV-IRES-eGFP vector by PCR amplification (eGFP forward primer, 5'-GCCACCATGGTGAGC-3'; eGFP reverse primer, 5'-TTACTTGTACAGCTCGTCC-3'). PCR analysis for TCR β chain and γ chain rearrangements was performed as described elsewhere.^{16,17}

Results

Nanog expression in hematopoietic cells

To determine whether Nanog might be involved in the maintenance of the HPC lineage, we first examined Nanog expression in both BM and thymic hematopoietic lineages (Figure 1A). We also analyzed the expression of Oct3/4 and Sox2 that in concert with Nanog are involved in maintenance of pluripotency of ES cells (Figure 1B).¹⁸ Although the level of Nanog expression in HPC populations is low compared with that in ES cells, we detected expression in the B-cell lineage (CD19⁺) and a subpopulation of the myeloid lineage (CD11b⁺ and Gr-1⁺). However, we could detect only a low level of Nanog expression in c-Kit⁺Sca1⁺Lineage⁻ stem cells (KSL cells; not fractionated by CD34) or T subpopulations in the thymus (Figure 1A). A low but significant level of Nanog expression was detected in the testis. In the thymus, Nanog expression remains very low throughout the double-negative (DN) stages, then increases at the double positive (DP) stage, and then decreases again in the CD4 and CD8 single-positive (SP) stages. In conclusion, Nanog expression is detectable in some HPC lineages, but the overall expression level is far lower than that in ES cells. Comparing with the expression level in ES cells, expression of Oct3/4 and Sox2 was barely detected in hematopoietic cell lineages.

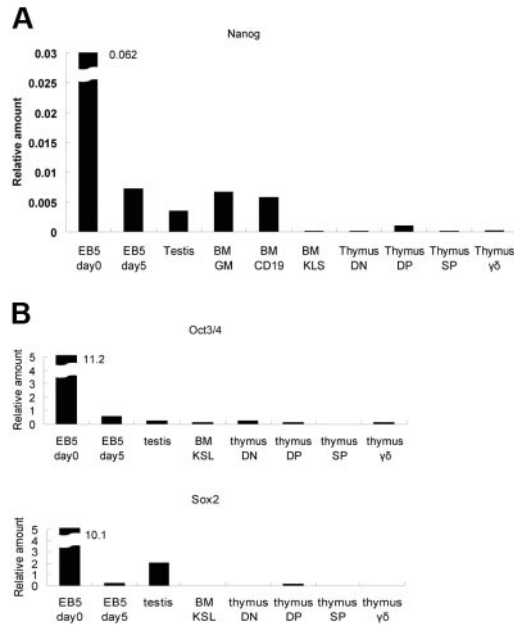


Figure 1. Expression of Nanog in hematopoietic cells. (A) Expression of Nanog in the indicated cell types was measured by quantitative reverse transcription polymerase chain reaction (QRT-PCR). (B) Expression of Oct3/4 and Sox2 in the indicated cell types was measured by QRT-PCR. The values were normalized using the *Gapdh*, *βactin*, and *HPRT* control genes. EB5 day 0, undifferentiated EB5 ES cell line¹⁹; EB5 day 5, EB5 ES cells that were cultured in the absence of LIF for 5 days; testis, unfractionated testis cells; BM GM, bone marrow cells expressing either Gr1 or Mac1; BM CD19, bone marrow cells expressing CD19; BM KSL, lineage negative bone marrow cells that express c-Kit and Sca-1; thymus DN, CD4⁻CD8⁻ thymocytes; thymus DP, CD4⁺CD8⁺ thymocytes; thymus SP, pooled CD4 SP and CD8 SP thymocytes; thymus $\gamma\delta$, $\gamma\delta$ T cells. This analysis was performed 3 times with similar results obtained in 2 other independent experiments.

Thymus disorder of recipients reconstituted with Nanog transduced hematopoietic stem cells

We next investigated the effect of Nanog overexpression on the differentiation of hematopoietic cells. For this purpose we transduced the *Nanog* gene into KSL cells using a retroviral vector and evaluated their capacity to reconstitute hematopoiesis in irradiated recipients. In this experiment, *Nanog*-transduced (*Nanog*) cells were detected by GFP expression driven by the retroviral vector.

Contrary to our expectation, the proportion of eGFP⁺ cells in host hematopoietic tissues receiving *Nanog* KSL cells is markedly lower than those in the hosts receiving control KSL cells. Interestingly, the eGFP⁺ population in the KSL fraction is lower than that in other fractions (data not shown). These results indicate that *Nanog* overexpression is not only ineffective in conferring any growth advantage to HSCs in the bone marrow but also inhibitory to their activity.

Surprisingly, however, the thymus of all recipients of *Nanog* KSL cells (*Nanog* T thymus, n > 50) were dominated almost completely by eGFP⁺ donor cells (Figure 2A), whereas the cellularity of the *Nanog* T thymus was markedly reduced (Figure 2B-C). The same phenotype was induced by transduction of *Nanog* into more mature CD34⁺ hematopoietic progenitors, suggesting noncommitment of the long-term reconstituting stem cells in this disorder (data not shown). The architecture of the normal thymus with an explicit distinction between the cortex and medulla was not recognizable by hematoxylin staining in the thymus of *Nanog* KSL cells. (Figure 2B). However, the 2 areas are still distinguishable by immunostaining with ER-TR4 and ER-TR5 markers, although the sizes of both areas are markedly reduced. Indeed, cells expressing

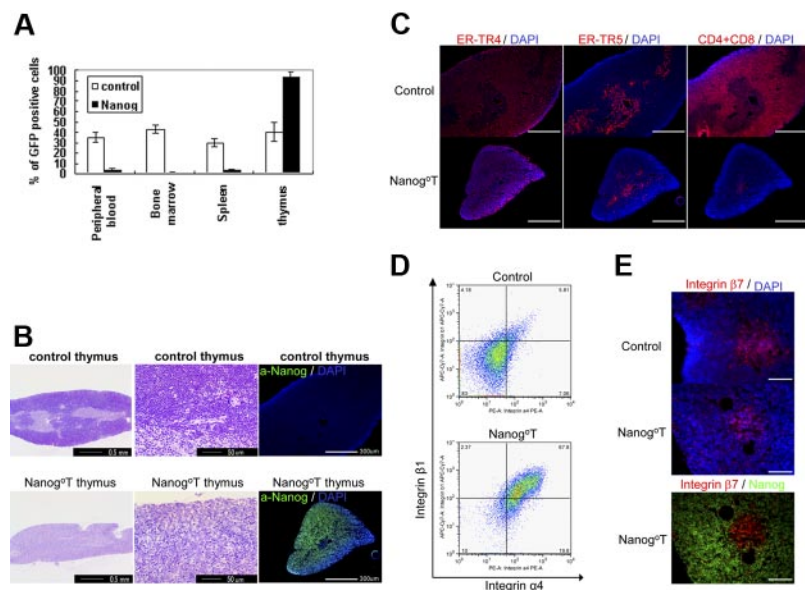


Figure 2. Effect of Nanog overexpression on the differentiation of hematopoietic cells. Irradiated mice were reconstituted KSL cells transduced either by *Gfp* gene alone or *Nanog-lers-Gfp*. Cells expressing the transgenes were distinguished by GFP expression. (A) Eight weeks later, the cells were harvested from various tissues of the recipients, and the proportion of GFP⁺ cells was measured by FACS. Compared with control recipients, the proportion of GFP⁺ cells in the peripheral blood, bone marrow, and spleen of the recipients remains at a low level. In contrast, nearly all cells in the thymus are GFP⁺. Bars represent a standard deviation. (B) Thymus atrophy in recipients of *Nanog* KSL cells (*Nanog*-thymus). Immunostaining by anti-*Nanog* antibody showed that *Nanog*-thymuses are occupied by cells expressing *Nanog*. The distinction of cortex and medulla, which is easily seen in the control thymus by hematoxylin staining, is difficult to discern in *Nanog* thymuses. The normal cortex of *Nanog* thymuses is replaced by lightly stained cells with larger cytoplasm. (C) Serial sections of thymuses were immunostained by antibodies to ER-TR4 and ER-TR5, which specify cortex and medulla, respectively. Thymocytes were also visualized by a mixture of antibodies to CD4 and CD8. Although the distinction between cortex and medulla is blurred as shown by HE staining, immunostaining by these antibodies demonstrate that each thymus compartment is preserved in the *Nanog*-thymus. In *Nanog*-thymuses, thymocytes expressing either CD4 or CD8 are present only in the medulla. Scale bar, 300 μ m. (D) Integrin α 4 and β 1 expression of the control T cells expressing GFP and *Nanog* T cells. Almost all *Nanog* T cells express integrin α 4 and integrin β 1, whereas only a small fraction of control thymocytes express it. FACS data of cells gated in GFP⁺ population is presented. (E) Integrin β 7 expression in *Nanog*-thymus. The expression of integrin β 7 was found only in the host T cells in the medulla of *Nanog*-thymus. However, *Nanog* expression is found in the cortex. Also in the control thymus, β 7⁺ cells are localized in the medulla. Scale bar, 100 μ m.

either CD4 or CD8 are present only in the medulla of Nanog thymuses, whereas they are present in both areas of control mice. Almost all Nanog T cells are a4b1, whereas this population is low in the T cells transduced with the control vector (Figure 2D). Although b7⁺ cells are found in the medulla of the thymus dominated by Nanog T cells, they are Nanog⁻ (Figure 2E). These observations suggest that the occupation of cortex region by Nanog T cells results in the reduction of host thymocytes and eventually atrophy of the thymus.

Perturbed T-cell differentiation by ectopic Nanog expression

We next characterized the Nanog T cells dominating the host thymus. Nanog T cells in the host thymus 4 months after the reconstitution consist of a rather homogeneous population that are $\gamma\delta$ TCR⁺, $\alpha\beta$ TCR⁻, CD8⁻, CD4⁻, CD44⁺, and CD25⁺. They express approximately a 2-fold higher level of Nanog than E14 ES cell lines,¹⁹ and do not express a significant level of Oct3/4 and Sox2 that are expressed in ES cells (data not shown). However, donor thymocytes (eGFP⁺) that were transduced with the eGFP gene alone consist of the same populations as those present in the normal thymus. Nanog overexpression supports preferential differentiation to $\gamma\delta$ T cells while decreasing the generation of $\alpha\beta$ T cells (Figure 3A). Consistent with this phenotype, genomic PCR analysis of TCR genes showed preferential rearrangement of $\gamma\delta$ TCRs. Nanog T cells harvested from 3 distinct thymi, no VJ β rearrangement was observed, whereas DJ β rearrangement was detected in 2. However, VJ γ rearrangement was observed in all samples, although the pattern of rearrangement is variable (Figure 3B).

Phenotype of the host thymus is characterized by atrophy and dominance of Nanog T cells. To gain some insights into this process, we investigated the composition of cells in the thymus at an earlier stage, 1 month after the reconstitution by Nanog KSL cells (Figure 3C). At this stage, the eGFP⁺ population is still a smaller fraction than eGFP⁻ cells. Among the eGFP⁺ fraction, both

eGFP^{dull} and eGFP^{high} cells were distinguished. Interestingly, the eGFP^{dull} population contains a considerable number of $\alpha\beta$ TCR⁺ cells, whereas eGFP^{high} cells are mostly $\gamma\delta$ TCR⁺ cells. This result indicates that, although $\alpha\beta$ TCR⁺ cells are generated from Nanog KSL cells, high Nanog expression may have some suppressive effect on generation of $\alpha\beta$ TCR⁺ cells. Indeed, we have never observed a single thymus dominated by $\alpha\beta$ TCR⁺ cells by reconstitution with Nanog KSL cells (n > 50). Thus, atrophic thymus occupied by $\gamma\delta$ TCR⁺ cells is an outcome of the Nanog overexpression in T-cell progenitors.

Transfer of thymus disorder by Nanog T cells

The thymus disorder displayed in hosts of Nanog KSL cells is likely to be ascribed to the generation of CD25⁺CD44⁺ $\gamma\delta$ TCR⁺ cells that cause the reduction of normal T cells, thereby resulting in the atrophy of the thymus. We next investigated whether the same disorder can be transferred to secondary hosts by the Nanog T cells that dominate the thymus of primary hosts. Nanog T cells were harvested from thymuses of mice that had been reconstituted with Nanog KSL cells. eGFP⁺ thymocytes (10⁶) were transferred intravenously to normal mice. As expected, thymuses of all recipient mice (n = 12) underwent atrophy and were occupied by Nanog T cells by 8 weeks after transfer (Figure 4). However, eGFP⁺ thymocytes derived from KSL cells transduced with eGFP gene alone could not be detected in the thymus of the secondary host. This result demonstrates clearly that Nanog T cells have an ability to home to the thymus and cause the reduction of host thymocytes. Despite such a remarkable effect on the host thymus, injection of Nanog T cells did not show any obvious effect in peripheral lymphoid tissues. In the secondary host, Nanog T cells were detected in the cortex but not in the medulla of the thymus or in any other lymphoid organs 2 months after transfer. Although mucosal tissues are the preferential homing destination for $\gamma\delta$ T

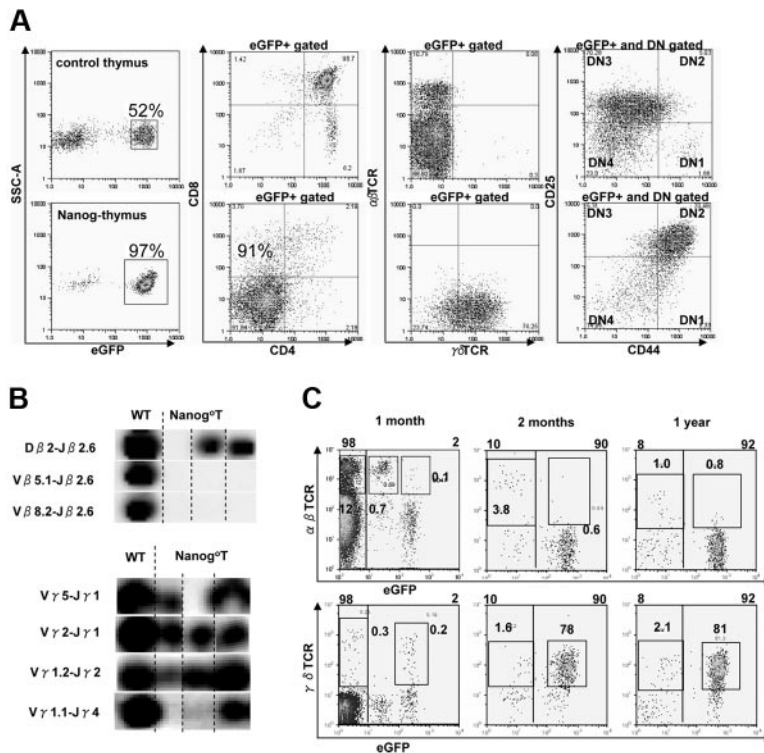


Figure 3. T-cell development by Nanog overexpression. (A) Characterization of T cells in Nanog-thymuses. Almost all (97%) cells in Nanog-thymuses are GFP⁺, whereas approximately half of the cells in the control thymus are GFP⁺. Nanog T cells are CD4⁻CD8⁻ (double negative, DN), CD44⁺CD25⁺, and $\gamma\delta$ TCR⁺. This phenotype is invariant in all independent experiments. The GFP⁺ cells in the control group consist of T cells from all normal stages. (B) TCR gene rearrangements in 3 clones of Nanog T cells that are isolated from the individual mice 4 months after the reconstitution. In contrast to TCR β DJ or TCR γ VJ rearrangements, TCR β V(D)J rearrangement was barely detected. We obtained similar results in 2 other independent experiments. The nomenclature of TCR γ segments is followed by the classification defined by Garman RD nomenclature.³⁷ (C) The time course of the occupancy of thymus by Nanog T cells. The phenotype and cellularity of thymus isolated from the Nanog KSL-reconstituted mice at 1 month, 2 months, and 1 year after reconstitution are shown.

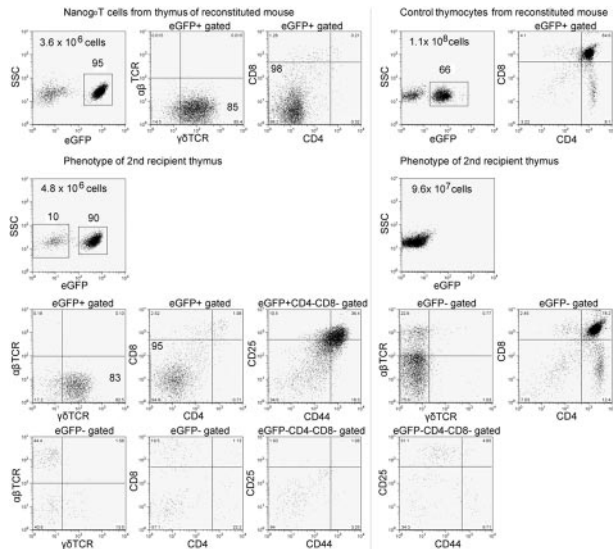


Figure 4. Transfer of the thymus disorder by Nanog T cells. Nanog T cells were generated in a recipient that was irradiated and reconstituted by Nanog KSL cells. Eight weeks later, eGFP⁺ cells were purified from the thymus, and 10⁵ cells were transferred to untreated secondary recipients. As a control, the same number of eGFP⁺ cells generated in the thymus of recipients reconstituted by KSL transduced with the control vector was transferred. The surface phenotype of eGFP⁺ cells in the primary recipients is shown in the upper panels. The chimerism of eGFP⁺ cells in secondary recipients is shown in the middle panels, and total cellularity of thymus is also shown. The surface phenotype of eGFP⁺ and eGFP⁻ cells in the thymus of the secondary recipients were also analyzed (bottom panels).

cells, virtually no eGFP⁺ cells were detected there (data not shown). Nanog T cells harvested from the thymus of the secondary host were CD25⁺CD44⁺ $\gamma\delta$ TCR⁺, suggesting that the basic features of Nanog T cells remained unchanged after transfer.

Sustained Notch-dependent growth of Nanog T cells on stromal cells

Nanog T cells express CXCR4, CCR7, CCR9, IL-7R, and c-Kit, the same set of receptors for chemokines and cytokines as those expressed in normal CD44⁺CD25⁺ thymocytes²⁰⁻²² (data not shown). To gain an insight into the dominance of Nanog T cells, we investigated the growth requirement of Nanog T cells. Like normal

thymocytes, Nanog T cells proliferate actively on OP9-DL1 but not on OP9. Hes1 that is induced by the Notch1 activation was detected in Nanog T cells cocultured with OP9-DL1 but not OP9. The cleaved Notch1 was also detected in Nanog T cells cocultured with OP9-DL1, and this expression is suppressed with DAPT, indicating that this is due to the action by γ -secretase. (Figure 5 A). Moreover, the growth of Nanog T cells on OP9-DL1 is suppressed by DAPT down to 50% of the untreated control (data not shown). All these results indicate that Notch 1 is essential for proliferation of Nanog T cells. Moreover, the proliferation of Nanog T cells on OP9-DL1 is faster than normal DN T cells. Thus, this difference in the growth rate may account for the overdominance of Nanog T cells.

Nanog T cells inhibit the earliest step of host T-cell development

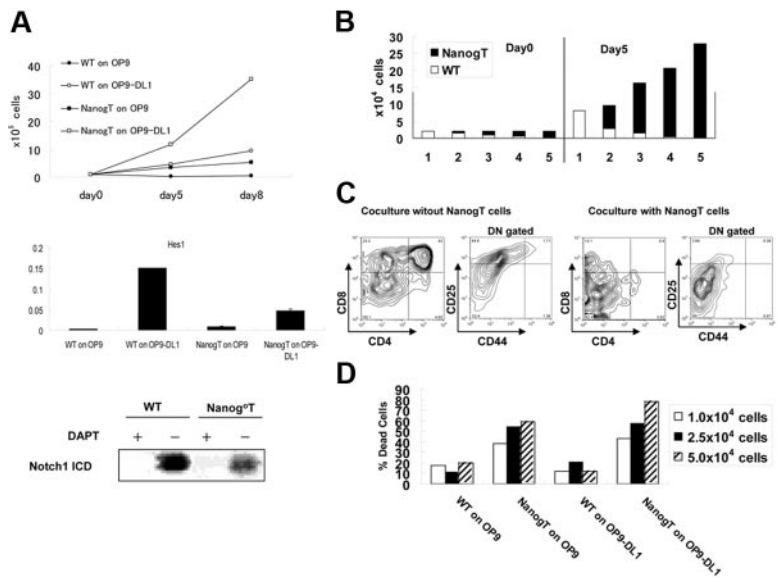
If the thymus microenvironment is affected by Nanog T cells, this can account, at least in part, for the suppression of normal T-cell development by the Nanog T cells. To specify the stage of host T cells that is affected by Nanog T cells, we have analyzed the surface phenotype of host thymocytes at various times after the transfer of 10⁵ Nanog T cells. FACS analysis revealed that the percentage of nontransduced thymocytes progressively decreased to around 90% between 6 (data not shown) and 8 (Figure 4) weeks after injection of Nanog T cells. It should be emphasized that, although Nanog T cells overwhelmed the host thymus, the total cellularity decreased to 10% at 8 weeks after the reconstitution. Hence, the reduction of the absolute number of host thymocytes should be more than 100-fold. FACS analysis of GFP⁻ cells remaining in the recipient thymus revealed a marked reduction of DP populations. Further analysis of DN population revealed a marked reduction of CD25⁺ population, indicating that Nanog T cells suppress T-cell development at stages earlier than DN2 (Figure 4).

Nanog T cells suppress stromal cell-dependent T-cell development in vitro

To further explore the mechanism underlying inhibition of T-cell development by Nanog T cells, we exploited in vitro culture of T cells on OP9-DL1 cells. Normal DN T cells and Nanog T cells were mixed at various ratios (1:3, 1:1, 3:1), and a total of 2 × 10⁴

Figure 5. Nanog T cells suppress stromal cell-dependent T-cell development in vitro.

(A) Notch signal-dependent growth of Nanog T cells in vitro. Upper panel shows the growth rate of Nanog T cells cocultured with OP9 or OP9-DL1. Middle panel shows the expression of Hes1 at day 5 of coculture. Lower panel shows the Western blotting for cleaved active Notch1. WT and Nanog T cells were cocultured on OP-DL1 with or without DAPT for 2 days. Cells (5 × 10⁵) were used for Western blotting. (B) Growth advantage of Nanog T cells on OP9-DL1. Wild-type (wt) DN thymocytes and Nanog T cells were mixed at varying ratios, and a total of 2 × 10⁴ cells were cultured on OP9-DL1. Five days later, all cells were harvested and GFP⁺ (filled column) and GFP⁻ (open column) lymphocytes were counted. The ratio of wild-type DN cells to Nanog T cells are (1) 1:0, (2) 3:1, (3) 1:1, (4) 1:3, and (5) 0:1. (C) Nanog T cells inhibit the differentiation of wild-type thymocytes in vitro. FACS analysis of GFP⁻ cells in cultures containing only wt cells or a 1:1 mixture of wt and Nanog thymocytes. In the absence of Nanog T cells, all stages of T-cell development from DN to SP cells were generated on OP9-DL1. However, differentiation of DP cells was markedly suppressed by coculture with Nanog T cells. DN gated means CD4⁻CD8⁻ gated. (D) Stromal cell damage induced by Nanog T cells. WT or Nanog thymocytes (10⁴, 2.5 × 10⁴, or 5.0 × 10⁴) were cultured on either OP9 or OP9-DL1 cells for 5 days. The proportion of live to dead stromal cells was determined by FACS of PI-stained cells. Stromal cells were distinguished from lymphocytes by their expression of DsRED.



cells were cultured on OP9-DL1 for 5 days. Regardless of the starting ratio of 2 populations, Nanog T cells grew 3 times more rapidly than normal DN thymocytes and eventually overwhelmed the normal DN T cells (Figure 5B). This higher proliferative ability of Nanog T cells may well account for the *in vivo* situation in which the host thymus is overwhelmed by Nanog T cells. The differentiation of DP cells from normal DN cells was severely affected by the presence of Nanog T cells also in this *in vitro* setting (Figure 5C). Moreover, CD25⁺ cells were extensively affected and reduced in DN population, consistent with *in vivo* data. The phenotype of thymus of the secondary recipients of Nanog T cells can be recapitulated in the coculture of normal DN cells and Nanog T cells on OP9-DL1. Taken together, Nanog T cells have not only a growth advantage over host thymocytes but also a suppressive activity on the development of host thymocytes.

Erosion of stromal cell layer by Nanog T cells *in vitro*

One interesting characteristic of Nanog T cells in the atrophic thymus is decreased expression of Notch1 and Hes1 (data not shown). However, as shown in Figure 5A, Nanog T cells proliferate actively in a Notch1-dependent manner. Thus, the low Notch1 expression may be due to the deficiency of host thymus at the atrophic stage. Of note is that the thymus atrophy is induced by Nanog T cells. A possible way to explain all such contradictory phenomena is to hypothesize that Nanog T cells may have an activity to destruct the microenvironment for the proliferation and development of DN fraction. This hypothesis can also explain the observation that the proliferation of Nanog T cells is limited in the host thymus. Consistent with this is *in vitro* observation that in all cultures of Nanog T cells, it is difficult to maintain the long-term growth of Nanog T cells, because of the erosion of the OP9-DL1 stromal layer (data not shown). Thus, we sought to determine whether stromal cell death is accelerated by Nanog T cells.

Nanog T cells or normal DN cells were cultured for 4 days on either OP9 or OP9-DL1, and the proportion of PI-stained stromal cells was measured by FACS (Figure 5D). Markedly higher proportions of stromal cells were stained by PI in cultures

containing Nanog T cells compared with those containing normal DN cells. Thus, Nanog T cells appear to have a toxic effect on stromal cells. This result is consistent with our hypothesis that low Notch1 expression in Nanog T cells in the host is due to loss of the stromal cell component that is required for maintenance of Notch1 expression.

Development of lymphoproliferative disorder from Nanog T cells in old mice

Finally, we investigated the long-term fate of mice that were reconstituted with Nanog KSL cells. More than a year after the reconstitution, we did not notice any significant changes in the behavior of mice. However, from 13 months after reconstitution, recipient mice started to die in succession. Thus, we decided to kill all remaining hosts (9 hosts derived from 3 independent transfer experiments) at 13.5 months for pathologic analysis. Splenomegaly and lymph node swelling were found in all mice. The thymus remained atrophic in all mice except one case in which the thymus was abnormally swollen. In this mouse, we observed abundant proliferation of Nanog T cells in the medulla which was never observed at earlier stages. Histologic analysis showed that the cells responsible for the hypertrophy of peripheral lymphoid tissues are Nanog T cells (eGFP⁺ cells), suggesting that this lymphoproliferative disorder is solely ascribed to the transformation of Nanog T cells (Figure 6A-B). Consistent with this, expression of $\gamma\delta$ TCR, CD25, and CD44 remained unchanged in all eGFP⁺ cells. eGFP⁺ cells were also found in circulation, suggesting that they have acquired leukemic properties. Unlike Nanog T cells in the thymus that were observed at early stages after transfer (2 months), Nanog T cells in the periphery and the thymus medulla express $\beta 7$ integrin, suggesting that additional events were required for the ability to grow in the periphery (Figure 6C). As shown in Figure 6B, the red pulp of spleen was infiltrated by Nanog T cells. Likewise, B-cell areas of the lymph nodes are eroded by Nanog T cells. Hence, like other leukemic cells, the transformed Nanog T cells diffusely infiltrate the peripheral lymphoid tissues, thereby destroying their architecture. Although Nanog T cells appear to be

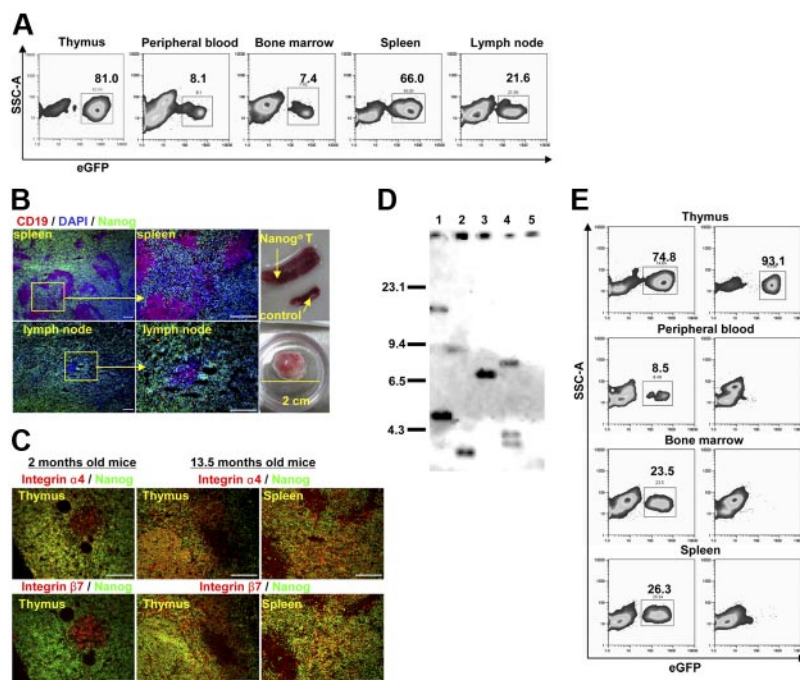


Figure 6. Oncogenic transformation of Nanog T cells. Mice were killed 13.5 months after irradiation and transfer of Nanog KSL cells. (A) In contrast to earlier stages after reconstitution, a significant number of GFP⁺ cells were detected in all peripheral tissues, including peripheral blood. (B) Splenomegaly and lymph node swelling were detected in all mice ($n = 9$). One lymph node had swollen to a huge mass. Nanog T cells infiltrate the spleen and lymph nodes diffusely leaving small islands of B cells (CD19⁺ cells). Scale bar, 100 μ m. (C) Unlike during the atrophic phase, expression of $\beta 7$ integrin was detected in considerable proportions of Nanog T cells in all peripheral tissue (thymus and spleen shown). Scale bar, 100 μ m. (D) Southern blot analysis of the MSCV integrations present in Nanog T cells derived from 4 distinct recipients (lane 1, atrophic phase; lanes 2-4, malignant phase). DNA (5 μ g) from each cell was digested with *EcoRI* and hybridized with a *egfp* probe isolated from the MSCV vector. Each band represents a separate MSCV integration. Lane 5 indicates WT thymocytes as a negative control. (E) Transformed cells in the periphery were transferred to second recipients. A diffuse infiltration of GFP⁺ cells was detected in all lymphoid tissues (thymus, peripheral blood, bone marrow, and spleen were shown in this figure) 2 weeks after transfer. Left panels show transfer of Nanog T cells at malignant phase; right panels show transfer of Nanog T cells at atrophic phase.

highly proliferative in the peripheral lymphoid tissues, their *in vitro* growth on OP9-DL1 was not different from that of Nanog T cells before transformation. So far, we could not obtain any evidence for generation of a gain-of-function mutation of Notch1 in Nanog T cells. Moreover, they maintained the ability to damage OP9-DL1. However, unlike Nanog T cells at earlier phases, they can home to the peripheral lymphoid tissues and proliferate on transfer. Thus, during the transformation process, Nanog T cells acquire $\beta 7$ integrin expression and the ability to proliferate in the peripheral lymphoid tissues.

We next investigated clonality of lymphoproliferative Nanog T cells by examining the insertion sites of the retrovirus vector using *egfp* gene as a probe. As expected, all tested lymphoproliferative cells appeared clonally selected, either monoclonal or biclonal (Figure 6D, lanes 2-4). However, such a selection has already been found before lymphoproliferative transformation (Figure 6D, lane 1). Thus, clonal selection takes place during the dominance of Nanog T cells.

We next investigated whether the lymphoproliferative disorder can be transferred to secondary hosts by the lymphoproliferative Nanog T cells which were purified from peripheral tissue of primary hosts. Lymphoproliferative Nanog T cells (10^6) were transferred intravenously to normal mice. As expected, infiltrations by lymphoproliferative Nanog T cells were detected in all lymphoid organs of all recipient mice ($n = 12$) by 2 weeks after transfer (Figure 6D). However, the transfer of Nanog T cells at atrophic phase did not show any immediate effect on the host peripheral lymphoid tissues, although all recipients eventually developed lymphoproliferative disorder after a long-term incubation (data not shown). These findings suggested that ectopic Nanog expression invariably results in a disorder with thymus atrophy and subsequent $\gamma\delta$ T-cell malignancy.

Discussion

Contrary to our initial aim of enhancing the self-renewal capacity of hematopoietic stem cells, overexpression of Nanog in the hematopoietic lineages results in the thymus disorder characterized by thymus atrophy and dominance with $\gamma\delta$ TCR⁺ cells that survive only in the thymic cortex, destroy their surrounding microenvironment, and eventually develop to malignancy.

In this work, we focused on the effect of Nanog on T-cell development, because the thymus is the only organ that is affected by the reconstitution of Nanog-transduced KSL cells. However, the fact that expression of Nanog in KSL cells drastically reduces the reconstituting activity indicates that Nanog expression disturbs the development of multiple cell lineages and has a potential to cause varying disorders of the hematopoietic lineages when expressed ectopically.

In T-cell development, overexpression of Nanog appears to affect the process of the development of DN T cells. In all independent experiments ($n > 50$), the thymus of host became atrophic and occupied by Nanog T cells with phenotype of $\gamma\delta$ TCR⁺, CD4⁻, CD8⁻, CD25⁺, and CD44⁺. This invariant phenotype suggests that expression of a high level of Nanog preferentially generate this unique $\gamma\delta$ TCR⁺ cells that are not present in normal tissues. Enhanced generation of $\gamma\delta$ TCR⁺ cell while suppressing that of $\alpha\beta$ TCR⁺ cells is the phenotype that is reminiscent of a conditional Notch signal KO in the T-cell lineage to some extent,²³⁻³⁰ suggesting that Nanog overexpression affects Notch signal in T-cell progenitors. However, that the

proliferation of Nanog T cells by themselves is dependent on Notch signal (Figure 5A) suggests that the Notch signal remains intact in Nanog T cells. In agreement with this conclusion, although severely suppressed, $\alpha\beta$ TCR⁺ cells were able to be detected in Nanog-expressing populations, particularly in Nanog^{dull} populations within 2 months after the reconstitution. Hence, molecular mechanisms underlying the dominance of $\gamma\delta$ TCR⁺ cells by Nanog overexpression may be due to a selective pressure in the host thymus and the advantage of Nanog T cells for survival rather than the cell autonomous defect in the Notch signal. Strong selective pressure is indeed noticed by the fact that Nanog T cells in the host thymus are already oligoclonal at 3 to 4 months of the reconstitution (Figure 6D). In fact, the emergence of a unique CD25⁺CD44⁺ $\gamma\delta$ TCR⁺ cell appears to be the sole cause of the disorder brought to the host, because the same abnormalities are reproduced by transferring Nanog T cells to a secondary recipient. Like normal DN cells, Nanog T cells can undergo proliferation on OP9-DL1. However, the proliferation rate of Nanog T cells on OP9-DL1 is higher than that of the normal DN cells. Thus, this difference in the growth rate may account for the domination of the host thymus by Nanog T cells (Figure 5A). Moreover, Nanog T cells by themselves have a deleterious effect on the cellular components comprising the microenvironment of the thymus cortex. The damage to the microenvironment not only inhibits the production of normal T cells but also limits the proliferation of Nanog T cells, resulting in thymus atrophy.

Although Nanog T cells grow more rapidly than normal DN cells, they do not develop to a lymphoproliferative disorder possibly because of damage to the thymic microenvironment. Indeed, over the period of a year, we could not detect any gross abnormality in the mice that received a BM transplant of Nanog-transduced hematopoietic stem cells. However, some mice started to die after a year, and we found swelling of peripheral lymphoid tissues in all mice at 13 months. This indicates that, although additional events are required for Nanog T cells to acquire the ability to undergo unlimited growth in the host, Nanog can be a candidate oncogene for some lymphoproliferative disorders. Indeed, in all cases with the lymphoproliferative disorder, we found that a significant number of circulating blood cells were Nanog T cells (Figure 6A), suggesting that a lymphoproliferative transition may have occurred, too. The most striking feature of Nanog T cells at the malignant phase is that such unlimited growth was only attained in the periphery, and the thymus remained often atrophic. In these mice, interestingly, even in the case with thymus enlargement, proliferating Nanog T cells were found in the thymus medulla that does not contain any Nanog T cells at earlier stages, whereas the cortex remained atrophic (Figure 6C). This suggests that the alteration of the homing destination from the cortex to the periphery is essential for the malignant transformation.

Before and after this event, Nanog T cells remained CD25⁺CD44⁺ $\gamma\delta$ TCR⁺. The proliferation of Nanog T cells requires Notch even after the malignant transformation, although cells grow faster after the transformation than before (data not shown). However, in all cases ($n = 8$), Nanog T cells in the periphery also express integrin $\alpha 4\beta 7$, which is not detected in Nanog T cells in the cortex during the thymus atrophy phase (Figure 6C). Integrin $\alpha 4\beta 7$ (LPAM-1) expressed in a subset of effector T cells or $\gamma\delta$ T cells in the intestine^{31,32} can mediate cell migration as a receptor for MAdCAM-1 and VCAM-1.³³⁻³⁵ Therefore, the expression of integrin $\beta 7$ in Nanog T cells

appears to be an essential event during the malignant transformation of Nanog T cells.

If ectopic expression of Nanog in human hematopoietic cells has the same effect as in mouse, one might suspect that Nanog may be involved in some $\gamma\delta$ T cells malignancies. To date, we have not found any report implicating Nanog in leukemia of mice or humans. In the mouse, however, leukemogenesis after irradiation induced thymus atrophy has been a popular model. Moreover, a line of evidence indicates the presence of $\gamma\delta$ T-cell malignancy in adult T-ALL (T-cell acute lymphoblastic leukemia)³⁶ that emerges after thymus atrophy. This group of T-ALL is $pT\alpha^+\gamma\delta TCR^+$, which is consistent with the phenotype of Nanog T cells that also express $pT\alpha$ (data not shown). Although, Nanog T cells are phenotypically distinct from this type of leukemia in terms of expression of CD4 and CD8 (data not shown), it would be interesting to further explore the possibility that $pT\alpha^+\gamma\delta TCR^+$ T-ALL of mice and humans includes a subtype in which ectopic expression of Nanog is involved in the disorder.

In conclusion, we show here that ectopic Nanog expression invariably results in a disorder with thymus atrophy and subsequent $\gamma\delta$ T-cell malignancy. Although Nanog is not involved in normal T-cell development, a further understanding of the Nanog-induced disorder of $\gamma\delta TCR^+$ cells should provide important insights into the process of lymphoproliferative disorder of T cells. During the submission of this paper, Nanog was reported to be expressed in both murine and human t(4;11)

leukemia cells.³⁸ This report supports our data that Nanog plays a role in an actual oncogenesis.

Acknowledgments

We thank Dr T. Amagai of Meiji College of Oriental Medicine for supplying ER-TR4 and ER-TR5 monoclonal antibodies; Dr J.C. Zuniga-Pflucker of the University of Toronto, Canada, for providing OP9-GFP and OP9-DL1 cells; Dr H. Hirata of FBRI and Dr H. Kurata of Cardio Inc for useful comment and technical advice; and Ms. Satomi Nishikawa of CDB for critical advice on experimental design.

This work was supported by CDB and partly by NEDO (grant "Focus 21 Healthy program utilizing regenerative medicine" 2002-2006).

Authorship

Contribution: Y.T. performed FACS analysis, immunostaining, qRT-PCR analysis, and reconstitution assay; T.E. performed retrovirus analysis; and S.N. and S.K. helped prepare the manuscript.

Conflict-of-interest disclosure: The authors declare no competing financial interests.

Correspondence: Shin Kawamata, Foundation for Biomedical Research and Innovation, 2-2 Chuo-ku, Minatojima Minamimachi Kobe 650-0047 Japan; email: kawamata@fbri.org.

References

- Niwa H, Miyazaki J, Smith AG. Quantitative expression of Oct-3/4 defines differentiation, dedifferentiation or self-renewal of ES cells. *Nat Genet.* 2000;24:372-376.
- Rossant J. Stem cells from the Mammalian blastocyst. *Stem Cells.* 2001;19:477-482.
- Avilion AA, Nicolis SK, Pevny LH, Perez L, Vivian N, Lovell-Badge R. Multipotent cell lineages in early mouse development depend on SOX2 function. *Genes Dev.* 2003;17:126-140.
- Chambers I, Colby D, Robertson M, et al. Functional expression cloning of Nanog, a pluripotency sustaining factor in embryonic stem cells. *Cell.* 2003;113:643-655.
- Mitsui K, Tokuzawa Y, Itoh H, et al. The homeoprotein Nanog is required for maintenance of pluripotency in mouse epiblast and ES cells. *Cell.* 2003;113:631-642.
- Tondreau T, Meuleman N, Delforge A, et al. Mesenchymal stem cells derived from CD133-positive cells in mobilized peripheral blood and cord blood: proliferation, Oct4 expression, and plasticity. *Stem Cells.* 2005;23:1105-1112.
- Romagnani P, Annunziato F, Liotta F, et al. CD14+CD34low cells with stem cell phenotypic and functional features are the major source of circulating endothelial progenitors. *Circ Res.* 2005;97:314-322.
- Hochedlinger K, Yamada Y, Beard C, Jaenisch R. Ectopic expression of Oct-4 blocks progenitor-cell differentiation and causes dysplasia in epithelial tissues. *Cell.* 2005;121:465-477.
- Antonchuk J, Sauvageau G, Humphries RK. HOXB4-induced expansion of adult hematopoietic stem cells ex vivo. *Cell.* 2002;109:39-45.
- Baba Y, Garrett KP, Kincade PW. Constitutively active beta-catenin confers multilineage differentiation potential on lymphoid and myeloid progenitors. *Immunity.* 2005;23:599-609.
- Dorsch M, Zheng G, Yowe D, et al. Ectopic expression of Delta4 impairs hematopoietic development and leads to lymphoproliferative disease. *Blood.* 2002;100:2046-2055.
- Kawamata S, Du C, Li K, Lavau C. Notch1 perturbation of hemopoiesis involves non-cell-autonomous modifications. *J Immunol.* 2002;168:1738-1745.
- Kunisato A, Chiba S, Nakagami-Yamaguchi E. HES-1 preserves purified hematopoietic stem cells ex vivo and accumulates side population cells in vivo. *Blood.* 2003;101:1777-1783.
- Van Vilet E, Melis M, Van Ewijk W. Monoclonal antibodies to stromal cell types of the mouse thymus. *Eur J Immunol.* 1984;14:524-529.
- Schmitt TM, Zuniga-Pflucker JC. Induction of T cell development from hematopoietic progenitor cells by delta-like-1 in vitro. *Immunity.* 2002;17:749-756.
- Durum SK, Candeias S, Nakajima H, et al. Interleukin 7 receptor control of T cell receptor gamma gene rearrangement: role of receptor-associated chains and locus accessibility. *J Exp Med.* 1998;188:2233-2241.
- Schlissel MS, Durum SD, Muegge K. The interleukin 7 receptor is required for T cell receptor gamma locus accessibility to the V(D)J recombinase. *J Exp Med.* 2000;191:1045-1050.
- Rodda DJ, Chew JL, Lim LH, et al. Transcriptional regulation of nanog by OCT4 and SOX2. *J Biol Chem.* 2005;280:24731-24737.
- Handyside AH, O'Neill GT, Jones M, Hooper ML. Use of BRL-conditioned medium in combination with feeder layers to isolate a diploid embryonic stem cell line. *Roux Arch Dev Biol.* 1989;198:48-55.
- Uehara S, Song K, Farber JM, Love PE. Characterization of CCR9 expression and CCL25/thymus-expressed chemokine responsiveness during T cell development: CD3(high)CD69+ thymocytes and gammadeltaTCR+ thymocytes preferentially respond to CCL25. *J Immunol.* 2002;168:134-142.
- Ueno T, Saito F, Gray DH. CCR7 signals are essential for cortex-medulla migration of developing thymocytes. *J Exp Med.* 2004;200:493-505.
- Plotkin J, Prockop SE, Lepique A, Petrie HT. Critical role for CXCR4 signaling in progenitor localization and T cell differentiation in the postnatal thymus. *J Immunol.* 2003;171:4521-4527.
- Washburn T, Schweighoffer E, Gridley T. Notch activity influences the alphabeta versus gammadelta T cell lineage decision. *Cell.* 1997;88:833-843.
- Huang EY, Gallegos AM, Richards SM, Lehar SM, Bevan MJ. Surface expression of Notch1 on thymocytes: correlation with the double-negative to double-positive transition. *J Immunol.* 2003;171:2296-2304.
- Yun TJ, Bevan MJ. Notch-regulated ankyrin-repeat protein inhibits Notch1 signaling: multiple Notch1 signaling pathways involved in T cell development. *J Immunol.* 2003;170:5834-5841.
- Tanigaki K, Tsuji M, Yamamoto N. Regulation of alphabeta/gammadelta T cell lineage commitment and peripheral T cell responses by Notch/RBP-J signaling. *Immunity.* 2004;20:611-622.
- Radtke F, Wilson A, Mancini SJ, MacDonald HR. Notch regulation of lymphocyte development and function. *Nat Immunol.* 2004;5:247-253.
- Pui JC, Allman D, Xu L. Notch1 expression in early lymphopoiesis influences B versus T lineage determination. *Immunity.* 1999;11:299-308.
- Kageyama R, Ohtsuka T, Tomita K. The bHLH gene Hes1 regulates differentiation of multiple cell types. *Mol Cells.* 2000;10:1-7.
- Rothenberg EV, Taghon T. Molecular genetics of T cell development. *Annu Rev Immunol.* 2005;23:601-649.
- Wilson E, Hedges JF, Butcher EC, Briskin M, Jutila MA. Bovine gamma delta T cell subsets

- express distinct patterns of chemokine responsiveness and adhesion molecules: a mechanism for tissue-specific gamma delta T cell subset accumulation. *J Immunol.* 2002;169:4970-4975.
32. Johansson-Lindbom B, Svensson M, Wurzel MA, et al. Selective generation of gut tropic T cells in gut-associated lymphoid tissue (GALT): requirement for GALT dendritic cells and adjuvant. *J Exp Med.* 2003;198:963-969.
33. Berlin C, Berg EL, Briskin MJ. Alpha 4 beta 7 integrin mediates lymphocyte binding to the mucosal vascular addressin MAdCAM-1. *Cell.* 1993;74:185-195.
34. Altevogt P, Hubbe M, Ruppert M, et al. The alpha 4 integrin chain is a ligand for alpha 4beta 7 and alpha 4 beta 1. *J Exp Med.* 1995;182:345-355.
35. Hilden TJ, Valmu L, Karkkainen S, Gahmberg CG. Threonine phosphorylation sites in the beta 2 and beta 7 leukocyte integrin polypeptides. *J Immunol.* 2003;170:4170-4177.
36. Asnafi V, Beldjord K, Boulanger E. Analysis of TCR, pT alpha, and RAG-1 in T-acute lymphoblastic leukemias improves understanding of early human T-lymphoid lineage commitment. *Blood.* 2003;101:2693-2703.
37. Garman RD, Doherty PJ, Raulet DH. Diversity rearrangement, and expression of murine T cell gamma genes. *Cell.* 1986;45:733-742.
38. Gausmann A, Wenger T, Eberle I, et al. Combined effects of the two reciprocal t(4;11) fusion proteins MLL*AF4 and AF4*MLL confer resistance to apoptosis, cell cycling capacity and growth transformation. *Oncogene.* 2007;26:3352-3363.